

Zak-OTFS and Turbo Signal Processing for Joint Sensing and Communication

Jinu Jayachandran, Muhammad Ubadah, Saif Khan Mohammed, Ronny Hadani, Ananthanarayanan Chockalingam and Robert Calderbank, *Fellow, IEEE*

Abstract—The Zak-OTFS input/output (I/O) relation is predictable and non-fading when the delay and Doppler periods are greater than the effective channel delay and Doppler spreads, a condition which we refer to as the crystallization condition. The filter taps can simply be read off from the response to a single Zak-OTFS pilot pulse, and the I/O relation can be reconstructed for a sampled system that operates under finite duration and bandwidth constraints. In previous work we had measured BER performance of a baseline system where we used separate Zak-OTFS subframes for sensing and data transmission. In this Letter we demonstrate how to use turbo signal processing to match BER performance of this baseline system when we integrate sensing and communication within the same Zak-OTFS subframe. The turbo decoder alternates between channel sensing using a noise-like waveform (spread pulse) and recovery of data transmitted using point pulses.

Index Terms—Zak-OTFS, Integrated Sensing and Communication, Turbo processing.

I. INTRODUCTION

6G propagation environments are changing the balance between time-frequency methods focused on OFDM signal processing and delay-Doppler methods (OTFS) [1]–[5]. OFDM is configured to prevent inter-carrier-interference (ICI) whereas OTFS is configured to embrace ICI [6]–[11]. In OFDM, once the I/O relation is known, equalization is relatively simple at least when there is no ICI. However, acquisition of the I/O relation is non-trivial and dependent on the accuracy of the assumed propagation model [12]. In contrast, equalization is more involved in OTFS due to inter-symbol-interference (ISI), however acquisition of the I/O relation is simple and model free [13]–[16]. Acquisition becomes more critical when Doppler spreads measured in KHz make it more and more difficult to estimate channels. The most challenging situation is the combination of unresolvable paths and high channel

spreads. In this Letter we present simulation results for a Veh-A channel [17] where the first three paths are not separable and cannot be estimated accurately.

In previous work [13], [14] we have described how to design a parametric family of pulse waveforms that can be matched to the delay and Doppler spreads of different propagation environments. A pulse is a signal in the time domain which realizes a quasi-periodic localized function on the DD domain. The prototypical structure of a pulse is a train of pulses modulated by a tone. We have analyzed performance in the situation when the pulse parameters matches the environment channel parameters, in the sense that, the delay period of the pulse is greater than the delay spread of the channel, and the Doppler period of the pulse is greater than the Doppler spread of the channel. We refer to this condition as the crystallization condition. We start from this baseline system where we dedicate separate Zak-OTFS subframes to channel estimation and data transmission, abbreviated as $S|C$ (sensing/channel estimation in the absence of communication signal) and $C|\bar{S}$ (communication in the absence of sensing signal).

The characteristic structure of a pulse is a train of pulses modulated by a tone, a signal with unattractive peak-to-average power ratio (PAPR). In more recent work [18] we have introduced the notion of filtering in the discrete delay-Doppler domain. We have described how to construct spread waveforms with desirable characteristics by applying a chirp filter in the discrete DD domain to a point pulse. One desirable characteristic is low PAPR, about 6dB for the exemplar spread pulse, compared with about 15dB for the point pulse. A second desirable characteristic is the ability to read off the I/O relation of the sampled communication system provided a second crystallization condition is satisfied. This work demonstrates how to integrate sensing and communication within a single Zak-OTFS subframe by combining a spread pulse for channel sensing with point pulses for data transmission. The filter in the discrete DD domain enables coexistence by minimizing interference between sensing and data transmission. We have demonstrated that sharing DD domain resources in this way increases effective throughput compared with traditional approaches that use guard bands to divide DD domain resources between sensing and communication.

In this Letter we demonstrate that turbo signal processing is able to close the performance gap between separate sensing and communication ($S|C$ and $C|\bar{S}$) and joint sensing and communication in the same Zak-OTFS subframe (which we

J. Jayachandran, M. Ubadah and S. K. Mohammed are with Department of Electrical Engineering, Indian Institute of Technology Delhi, India (E-mail: Jinu.Jayachandran@ee.iitd.ac.in, Muhammad.Ubadah@ee.iitd.ac.in, saifk-mohammed@gmail.com). S. K. Mohammed is also associated with Bharti School of Telecom. Technology and Management (BSTTM), IIT Delhi. R. Hadani is with Department of Mathematics, University of Texas at Austin, TX, USA (E-mail: hadani@math.utexas.edu). A. Chockalingam is with Department of Electrical Communication Engineering, Indian Institute of Science Bangalore, India (E-mail: achockal@iisc.ac.in). R. Calderbank is with Department of Electrical and Computer Engineering, Duke University, USA (E-mail: robert.calderbank@duke.edu).

The work of S. K. Mohammed was supported in part by the Jai Gupta Chair at I.I.T. Delhi, and also in part by a project at BSTTM funded by Bharti Airtel Limited.

This work has been submitted to the IEEE for possible publication. Copyright may be transferred without notice, after which this version may no longer be accessible.

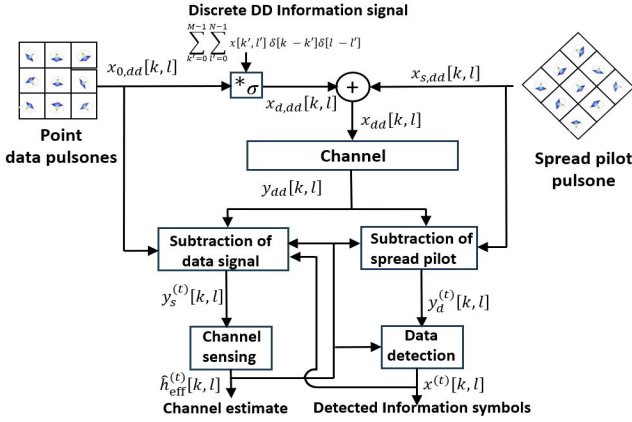


Fig. 1. Signal processing for proposed Zak-OTFS based iterative joint sensing and communication.

abbreviate as $S|C$ and $C|S$). The turbo principle of iterating between functional blocks in communication receivers has proven to be a powerful method of improving performance. For example, turbo iterations between channel equalizer and channel decoder have been shown to yield tremendous improvements in bit error performance [19], [20]. Likewise, iterations between channel estimation and turbo equalizer have been shown to improve the channel estimate over the iterations by using soft information fed back from the decoder from the previous iteration to generate extended training sequences between the actual transmitted training sequences [21]. In joint sensing and communication, we estimate the effective channel, then estimate the received spread pilot, then recover the data after subtracting our estimate for the received pilot from the received signal (see Fig. 1). The residual pilot (after cancellation) interferes with data transmission. In the turbo iteration, we take the estimated data, then estimate the received data signal, then improve our estimate for the effective channel by subtracting our estimate for the received data signal from the received signal. We show that five turbo iterations suffice to match the performance of separate sensing and communication across a wide range of Doppler shifts.

II. SYSTEM MODEL

In previous work [18] we have introduced a framework for joint sensing and communication where the pilot/sensing signal and the data signal are embedded in a single Zak-OTFS subframe. We recall [18] that Zak-OTFS carrier waveforms are quasi-periodic functions in the discrete DD domain with period M along the discrete delay axis and period N along the discrete Doppler axis. The superposition of pilot and data signals in the discrete DD domain is given by

$$x_{dd}[k, l] = \sqrt{E_d} x_{d,dd}[k, l] + \sqrt{E_p} x_{s,dd}[k, l] \quad (1)$$

where E_p denotes the energy of the pilot and E_d the energy of the data signal. The ratio E_p/E_d is therefore the pilot to data power ratio (PDR). The data signal $x_{d,dd}[k, l]$, $k, l \in \mathbb{Z}$ is given by

$$x_{d,dd}[k, l] = \frac{1}{\sqrt{MN}} x[k \bmod M, l \bmod N] e^{j2\pi \frac{k}{M} l}, \quad (2)$$

where each of the MN information symbols $x[k, l]$, $k = 0, \dots, M-1$, $l = 0, 1, \dots, N-1$ have average energy $\mathbb{E}[|x[k, l]|^2] = 1$. The exponential phase term in (2) renders $x_{d,dd}[k, l]$ quasi-periodic. For all $n, m \in \mathbb{Z}$

$$x_{d,dd}[k + nM, l + mN] = e^{j2\pi \frac{n l}{N}} x_{d,dd}[k, l]. \quad (3)$$

The data signal in (1) can also be expressed in terms of filtering (in the DD domain) a quasi-periodic DD domain pulse at the origin.

$$x_{d,dd}[k, l] = \left[\begin{aligned} & \left(\sum_{k'=0}^{M-1} \sum_{l'=0}^{N-1} x[k', l'] \delta[k - k'] \delta[l - l'] \right) \\ & *_{\sigma} x_{0,dd}[k, l] \end{aligned} \right], \quad (4)$$

where

$$x_{0,dd}[k, l] \triangleq \sum_{n, m \in \mathbb{Z}} \delta[k - nM] \delta[l - mN] \quad (5)$$

is the data pulsone corresponding to a DD pulse at the origin. DD domain filtering is implemented through twisted convolution $*_{\sigma}$ and the filter taps in (4) depend on the information symbols. The pilot signal in (1) is given by

$$x_{s,dd}[k, l] = w_s[k, l] *_{\sigma} x_{p,dd}[k, l], \quad (6)$$

where the spreading filter $w_s[k, l]$ acts on the point pilot $x_{p,dd}[k, l]$ by twisted convolution. We follow [18] by considering chirp filters, where for $k = 0, 1, \dots, M-1$, $l = 0, 1, \dots, N-1$

$$w_s[k, l] = \frac{1}{MN} e^{j2\pi \frac{q(k^2 + l^2)}{MN}}, \quad (7)$$

and we refer to $q \in \mathbb{Z}$ as the slope parameter. The point pilot $x_{p,dd}[k, l]$ appearing in (6) is a discrete DD domain quasi-periodic impulse located at (k_p, l_p) and is given by

$$x_{p,dd}[k, l] = \sum_{n, m \in \mathbb{Z}} e^{j2\pi \frac{n l_p}{N}} \delta[k - k_p - nM] \delta[l - l_p - mN] \quad (8)$$

We then *lift* the discrete DD domain signal $x_{dd}[k, l]$ given by (1) to obtain a *continuous* DD domain signal

$$x_{dd}(\tau, \nu) = \sum_{k, l \in \mathbb{Z}} x_{dd}[k, l] \delta(\tau - k\tau_p/M) \delta(\nu - l\nu_p/N) \quad (9)$$

that is quasi-periodic with delay period τ_p and Doppler period $\nu_p = 1/\tau_p$. We then apply a pulse shaping filter $w_{tx}(\tau, \nu)$ to limit the transmitted TD signal to the duration and bandwidth of the Zak-OTFS subframe. This TD signal is obtained by applying the inverse Zak transform to the filtered DD domain signal $w_{tx}(\tau, \nu) *_{\sigma} x_{dd}(\tau, \nu)$.

Matched filtering at the receiver using $w_{rx}(\tau, \nu) = w_{tx}^*(-\tau, -\nu) e^{j2\pi\nu\tau}$ followed by sampling on the information grid results in the discrete DD domain signal given by

$$y_{dd}[k, l] = \underbrace{\sqrt{E_d} h_{\text{eff}}[k, l] *_{\sigma} x_{d,dd}[k, l]}_{\text{Rx. data signal}} + \underbrace{\sqrt{E_p} h_{\text{eff}}[k, l] *_{\sigma} x_{s,dd}[k, l]}_{\text{Rx. sensing/pilot signal}} + n_{dd}[k, l], \quad (10)$$

$$\hat{y}_{\text{d,dd}}^{(t)}[k, l] = \hat{h}_{\text{eff}}^{(t-1)}[k, l] *_{\sigma} \left[\sum_{k'=0}^{M-1} \sum_{l'=0}^{N-1} \hat{x}^{(t-1)}[k', l'] \delta[k - k'] \delta[l - l'] *_{\sigma} x_{0,\text{dd}}[k, l] \right]. \quad (14)$$

where $n_{\text{dd}}[k, l]$ represents noise in the discrete DD domain. Note that it is associativity of twisted convolution that allows us to represent a cascade of filters/channels as a single effective channel filter $h_{\text{eff}}[k, l]$. In our previous work [18] we have described how the receiver senses the channel (estimates $h_{\text{eff}}[k, l]$) from the cross-ambiguity $A_{y, x_s}[k, l]$ between $y_{\text{dd}}[k, l]$ and the transmitted spread pilot $x_{\text{s,dd}}[k, l]$. We recall (Theorem 3 from [18]) that

$$\begin{aligned} A_{y, x_s}[k, l] &= \sqrt{E_p} h_{\text{eff}}[k, l] *_{\sigma} A_{x_s, x_s}[k, l] \\ &+ \sqrt{E_d} h_{\text{eff}}[k, l] *_{\sigma} A_{x_d, x_s}[k, l] + A_{n, x_s}[k, l], \end{aligned} \quad (11)$$

where $A_{x_s, x_s}[k, l]$ is the self-ambiguity function of the spread pilot signal, $A_{x_d, x_s}[k, l]$ and $A_{n, x_s}[k, l]$ are the cross-ambiguity functions of the transmitted data signal $x_{\text{d,dd}}[k, l]$ and noise signal $n_{\text{dd}}[k, l]$ respectively with the spread pilot signal.

The self-ambiguity function of the point pilot $x_{\text{p,dd}}[k, l]$ is supported on the *period lattice* Λ_p comprising integer linear combinations of $(\tau_p, 0)$ and $(0, \nu_p)$.

We have shown [18] that the self-ambiguity function of the spread pilot is supported on a lattice Λ obtained by rotating Λ_p . Let \mathcal{S} denote the support region of the effective channel in the discrete DD domain. The crystallization conditions with respect to the lattice Λ are satisfied if the translates of \mathcal{S} by lattice points in Λ are disjoint. In this case, we can obtain the effective channel tap $h_{\text{eff}}[k, l]$ by evaluating the first term of (11) at points (k, l) in a fundamental domain of Λ . The second term in (11) represents interference to sensing from data. We recall (Theorem 4 from [18]) that the magnitudes $|A_{x_d, x_s}[k, l]|$ are essentially independent of k, l so that interference from data to sensing is noise-like (see also Fig.18 from [18]). The third term in (11) represents interference to sensing from noise. We recall (Appendix J from [18]) that $A_{n, x_s}[k, l]$ is zero-mean Gaussian distributed with variance essentially independent of k, l . Our estimate of $h_{\text{eff}}[k, l]$ is then

$$\hat{h}_{\text{eff}}[k, l] = \frac{A_{y, x_s}[k, l]}{\sqrt{E_p}} \text{ for } (k, l) \in \mathcal{S}. \quad (12)$$

We suppose that the crystallization conditions are also satisfied with respect to the lattice Λ_p . We use the estimate (12) to cancel the contribution made by the pilot to the received DD signal. After cancellation, the signal

$$y_{\text{dd}}[k, l] - \sqrt{E_p} \hat{h}_{\text{eff}}[k, l] *_{\sigma} x_{\text{s,dd}}[k, l]. \quad (13)$$

is used to recover the data using the matrix-vector formulation of the Zak-OTFS I/O relation (see [14] for details). By spreading the pilot signal, we integrate sensing and communication within the same Zak-OTFS subframe. Sharing DD domain resources in this way increases effective throughput compared

with traditional approaches that use guard bands to divide DD domain resources between sensing and communication (see Fig.28 from [18]). Spreading also reduces the PAPR of the pilot signal to about 5 dB compared with 15 dB for the original point pilot (see Fig.10 and Fig.11 from [18]).

We recall that integrated sensing and communication with spread pilots results in an uncoded 4-QAM BER of about 10^{-2} , compared with 10^{-5} for sensing and communication in separate Zak-OTFS subframes (see Fig.26 from [18]). The difference is three orders of magnitude. Section III describes a turbo signal processing method that is able to close this gap.

III. ITERATIVE SENSING AND COMMUNICATION

In this Section we describe the iterative signal processing algorithm illustrated in Fig. 1. The first iteration is described in Section II and the t^{th} iteration consists of four steps.

STEP 1: Inputs are the detected information symbols $\hat{x}^{(t-1)}[k, l]$, $k = 0, 1, \dots, M-1$, $l = 0, 1, \dots, N-1$ and estimated channel filter taps $\hat{h}_{\text{eff}}^{(t-1)}[k, l]$, $(k, l) \in \mathcal{S}$ from iteration $t-1$. We form $\hat{y}_{\text{d,dd}}^{(t)}[k, l]$ (see (14) at top of page) and subtract this estimate for the received data signal from the received signal to obtain

$$y_s^{(t)}[k, l] = y_{\text{dd}}[k, l] - \hat{y}_{\text{d,dd}}^{(t)}[k, l]. \quad (15)$$

The output $y_s^{(t)}[k, l]$ is a *data cancelled signal* that approximates the received spread pilot.

STEP 2: We use (12) to form the t^{th} estimate $\hat{h}_{\text{eff}}^{(t)}[k, l]$ for the effective channel filter taps

$$\hat{h}_{\text{eff}}^{(t)}[k, l] = \frac{A_{y_s^{(t)}, x_s}[k, l]}{\sqrt{E_p}} \text{ for } (k, l) \in \mathcal{S}. \quad (16)$$

STEP 3: We use $\hat{h}_{\text{eff}}^{(t)}[k, l]$, $(k, l) \in \mathcal{S}$ to form the t^{th} estimate $\hat{y}_{\text{s,dd}}^{(t)}[k, l]$ of the received pilot signal using

$$\hat{y}_{\text{s,dd}}^{(t)}[k, l] = \hat{h}_{\text{eff}}^{(t)}[k, l] *_{\sigma} x_{\text{s,dd}}[k, l]. \quad (17)$$

We subtract this estimate from the received signal to obtain

$$y_d^{(t)}[k, l] = y_{\text{dd}}[k, l] - \hat{y}_{\text{s,dd}}^{(t)}[k, l]. \quad (18)$$

This output is a *pilot cancelled signal* that approximates the received data signal.

STEP 4: We detect data/information symbols $\hat{x}^{(t)}[k, l]$ from $y_d^{(t)}[k, l]$ using the method described in Section II. We then move to STEP 1 of iteration $t+1$, and the algorithm halts after a fixed number of iterations.

Section IV presents numerical simulations illustrating that multiple iterations improve the fidelity of the *data cancelled* and *pilot cancelled* signals.

TABLE I
POWER-DELAY PROFILE OF VEH-A CHANNEL MODEL

Path number (i)	1	2	3	4	5	6
τ_i (μ s)	0	0.31	0.71	1.09	1.73	2.51
Relative power (p_i) dB	0	-1	-9	-10	-15	-20

IV. NUMERICAL SIMULATIONS

This Section reports simulation results for the Veh-A channel model [17] which consists of six channel paths. The channel gains h_i are modeled as independent zero-mean complex circularly symmetric Gaussian random variables, normalized so that $\sum_{i=1}^6 \mathbb{E}[|h_i|^2] = 1$. Table I lists the power-delay profile for the six channel paths. The Doppler shift of the i -th path is modeled as $\nu_i = \nu_{max} \cos(\theta_i)$, where ν_{max} is the maximum Doppler shift of any path, and the variables θ_i , $i = 1, 2, \dots, 6$, are independent and distributed uniformly in $[-\pi, \pi)$.

We consider Zak-OTFS modulation with Doppler period $\nu_p = 30$ KHz, delay period $\tau_p = 1/\nu_p = 33.3$ ms, $M = 31$ and $N = 37$. The channel bandwidth $B = M\nu_p = 0.93$ MHz and the subframe duration $T = N\tau_p = 1.2$ ms. Note that the first three channel paths introduce delay shifts in the interval $[0, 0.71]$ ms and each is less than the delay resolution. We consider matched filtering using root raised cosine (RRC) pulse shaping filters with roll-off factors $\beta_\nu = \beta_\tau = 0.6$. This increases the subframe duration to $T' = (1 + \beta_\nu)T = 1.92$ ms and the bandwidth to $B' = (1 + \beta_\tau)B = 1.40$ MHz. We consider a spread pilot pulse constructed using a chirp filter in the discrete delay-Doppler domain ((7) with $q = 3$) as described in [18]. We implement the turbo signal processing pipeline illustrated in Fig. 1 using MMSE equalization to recover information symbols using the effective channel matrix.

For a fixed data SNR of 25 dB we set the PDR to 10 dB so that the pilot power is sufficient to start the turbo process. Fig. 2 illustrates that in the crystalline regime, five turbo iterations (dashed curve with red triangles) are sufficient to match the BER performance of separate sensing and communications (dashed curve with black squares). When $\nu_{max} > 12$ KHz the estimate of the effective channel becomes less accurate because of Doppler domain aliasing, and BER performance degrades because interference from the residual pilot becomes more significant than noise. We focus on the role of channel estimation by designing a reference system (solid blue curve with diamonds) where sensing takes place in a separate subframe ($S|\bar{C}$) but data transmission is still subject to interference from the residual pilot ($C|S$). Fig. 2 illustrates that BER performance with five turbo iterations differs from that of the reference system by a small SNR offset.

Next we consider how BER performance depends on PDR, and we set $\nu_{max} = 6$ KHz so that we are operating deep in the interior of the crystalline regime. Fig. 3 illustrates that when $PDR < -10$ dB the pilot power is not sufficient to start the turbo process, that the initial estimate of the effective channel is not sufficiently accurate. When $PDR > 25$ dB interference from the residual pilot (after cancellation) is more significant than noise, and BER degrades as PDR increases. For intermediate values of the PDR, BER performance improves with

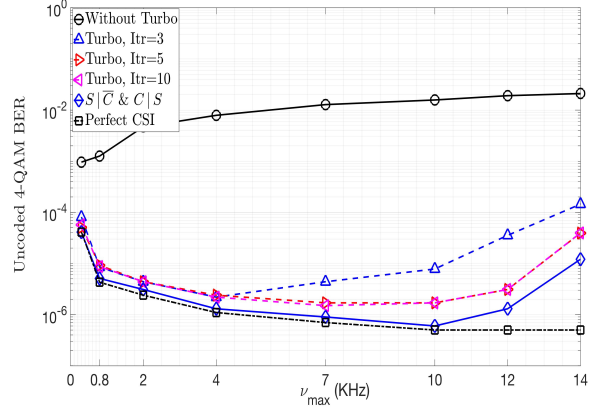


Fig. 2. Uncoded 4-QAM BER as a function of increasing ν_{max} . Veh-A channel, data SNR = 25 dB, PDR = 10 dB, Doppler period $\nu_p = 30$ KHz, $M = 31$, $N = 37$, RRC pulse shaping filter ($\beta_\nu = \beta_\tau = 0.6$).

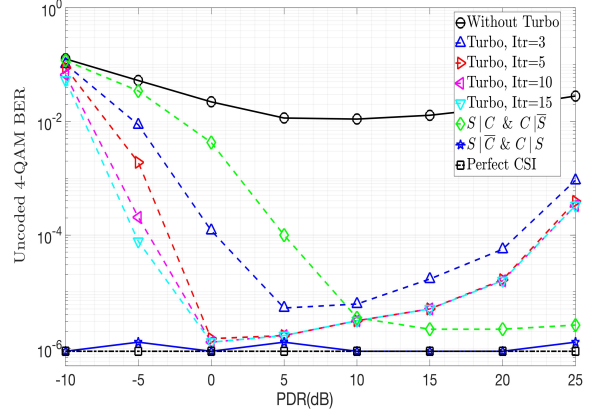


Fig. 3. Uncoded 4-QAM BER as a function of increasing PDR. Veh-A channel considered in Fig. 2.

increasing PDR as estimates of the effective channel become more accurate. This explains the characteristic “U” shape of the intermediate curves in Fig. 3. Again, we focus on the role of channel estimation by considering the reference system described above ($S|\bar{C}$ and $C|S$), where the residual pilot has very little energy and interference offered to the transmitted data is inconsequential (channel estimation is very accurate since it is based on a separate sensing-only subframe). We also consider a second reference system (green diamond), where sensing is subject to interference from data ($S|C$), but data recovery is not subject to interference from a residual pilot ($C|\bar{S}$). Data is transmitted in a separate subframe and there are no turbo iterations for this second reference system. Fig. 3 confirms that interference from the residual pilot is responsible for the degradation in BER performance with increasing PDR.

V. CONCLUSIONS

We started by observing that the uncoded 4-QAM BER performance of sensing and communications in separate Zak-OTFS subframes is three orders of magnitude better than that of integrated sensing and communication with spread pilots. In joint sensing and communication, we estimate the effective channel, then estimate the received spread pilot, then recover the data after subtracting our estimate for the

received pilot from the received signal. The residual pilot (after cancellation) interferes with data transmission, and we showed that this is the reason for the three orders of magnitude gap in performance. We described a turbo signal processing algorithm that alternates between channel sensing using a spread pilot and data recovery. We showed that five turbo iterations suffice to match the performance of separate sensing and communication across a broad range of Doppler shifts.

REFERENCES

- [1] H. Tataria, M. Shafi, A. F. Molisch, M. Dohler, H. Sjöland, and F. Tufveson, "6G wireless systems: Vision, requirements, challenges, insights, and opportunities," *Proceedings of the IEEE*, vol. 109, no. 7, pp. 1166-1199, Jul. 2021.
- [2] C. -X. Wang, X. You, X. Gao, X. Zhu, Z. Li, C. Zhang, H. Wang, Y. Huang, Y. Chen, H. Haas, J. S. Thompson, E. G. Larsson, M. Di Renzo, W. Tong, P. Zhu, X. Shen, H. V. Poor, and L. Hanzo, "On the road to 6G: Visions, requirements, key technologies, and testbeds," *IEEE Commun. Surveys & Tuts.*, vol. 25, no. 2, pp. 905-974, 2023.
- [3] R. Hadani et al., "Orthogonal time frequency space modulation," *Proc. IEEE WCNC'2017*, pp. 1-6, Mar. 2017.
- [4] Z. Wei, W. Yuan, S. Li, J. Yuan, G. Bharatula, R. Hadani and L. Hanzo, "Orthogonal time-frequency space modulation: a promising next-generation waveform," *IEEE Wireless Commun. Mag.*, vol. 28, no. 4, pp. 136-144, Aug. 2021.
- [5] W. Yuan et al., "Best readings in orthogonal time frequency space (OTFS) and delay Doppler signal processing," Jun. 2022. <https://www.comsoc.org/publications/best-readings/orthogonal-time-frequency-space-otfs-and-delay-doppler-signal-processing>.
- [6] A. Monk, R. Hadani, M. Tsatsanis, and S. Rakib, "OTFS - orthogonal time frequency space: a novel modulation meeting 5G high mobility and massive MIMO challenges," arXiv:1608.02993 [cs.IT] 9 Aug. 2016.
- [7] P. Raviteja, K. T. Phan, Y. Hong, and E. Viterbo, "Embedded pilot aided channel estimation for OTFS in delay-Doppler channels," *IEEE Trans. Veh. Tech.*, vol. 68, no. 5, pp. 4906-4917, May 2019.
- [8] P. Raviteja, Y. Hong, E. Viterbo, and E. Biglieri, "Practical pulse-shaping waveforms for reduced-cyclic-prefix OTFS," *IEEE Trans. Veh. Tech.*, vol. 68, no. 1, pp. 957-961, Jan. 2019.
- [9] C. Shen, J. Yuan, and H. Lin, "Error performance of rectangular pulse-shaped OTFS with practical receivers," *IEEE Wireless Commun. Lett.*, vol. 11, no. 12, pp. 2690-2694, Dec. 2022.
- [10] S. K. Mohammed, "Derivation of OTFS modulation from first principles," *IEEE Trans. Veh. Tech.*, vol. 70, no. 8, pp. 7619-7636, Aug. 2021.
- [11] S. K. Mohammed, "Time-domain to delay-Doppler domain conversion of OTFS signals in very high mobility scenarios," *IEEE Trans. Veh. Tech.*, vol. 70, no. 6, pp. 6178-6183, Jun. 2021.
- [12] E. Panayirci, H. Senol, and H. V. Poor, "Joint channel estimation, equalization, and data detection for OFDM systems in the presence of very high mobility," *IEEE Trans. Signal Process.*, vol. 58, no. 8, pp. 4225-4238, Aug. 2010.
- [13] S. K. Mohammed, R. Hadani, A. Chockalingam, and R. Calderbank, "OTFS – A mathematical foundation for communication and radar sensing in the delay-Doppler domain," *IEEE BITS the Information Theory Magazine*, vol. 2, no. 2, pp. 36-55, 1 Nov. 2022.
- [14] S. K. Mohammed, R. Hadani, A. Chockalingam, and R. Calderbank, "OTFS – Predictability in the delay-Doppler domain and its value to communications and radar sensing," *IEEE BITS the Information Theory Magazine*, IEEE early access, doi: 10.1109/MBITS.2023.3319595, Sep. 2023.
- [15] S. Li, W. Yuan, Z. Wei, J. Yuan, B. Bai, and G. Caire, "On the pulse shaping for delay-Doppler communications," *IEEE GLOBECOM'2023*, pp. 4909-4914, Dec. 2023.
- [16] S. Gopalam, I. B. Collings, S. V. Hanly, H. Inaltekin, S. R. B. Pillai, and P. Whiting, "Zak-OTFS implementation via time and frequency windowing," *IEEE Trans. Commun.*, IEEE early access, doi: 10.1109/TCOMM.2024.3366403.
- [17] ITU-R M.1225, "Guidelines for evaluation of radio transmission technologies for IMT-2000," *International Telecommunication Union Radio communication*, 1997.
- [18] M. Ubadah, S. K. Mohammed, R. Hadani, S. Kons, A. Chockalingam, and R. Calderbank, "Zak-OTFS for integration of sensing and communication," available online: arXiv:2404.04182v1 [eess.SP] 5 Apr 2024.
- [19] C. Douillard et al., "Iterative correction of intersymbol interference: turbo-equalization," *Eur. Trans. Telecommun.*, vol. 6, pp. 507-511, Sep.-Oct. 1995.
- [20] M. Tüchler, R. Koetter, and A. C. Singer, "Turbo equalization: principles and new results," *IEEE Trans. Commun.*, vol. 50, no. 5, pp. 754-767, May 2002.
- [21] R. Otnes and M. Tüchler, "Iterative channel estimation for turbo equalization of time varying frequency selective channels," *IEEE Trans. Wireless Commun.*, vol. 3, pp. 1918-1923, Nov. 2004.